nature food

Article

https://doi.org/10.1038/s43016-026-01452-8

Wheat yield sensitivity to compound hot–dry–windy events is increasing in China

Received: 6 December 2024

Accepted: 6 October 2026

Published online: 02 November 2026

Check for updates

Tengcong Jiang[1,2] ✉, Bin Wang[3,4,5], Zhihao He[1], Xiaoya Ru[6], Ning Yao[7], Kaiyuan Gong[7], Jianqiang He[7], Hao Feng[1,7], Qiang Yu[1,2] ✉ & Haijiao Ma[8] ✉

Compound hot–dry–windy events (HDWs) increasingly threaten wheat production, but temporal changes in wheat sensitivity remain unclear. Here we combined multidecadal county-level yield records, hourly reanalysis climate data, phenological observations and production-cost records to quantify responses to three HDW types across China. High-temperature, low-humidity events increased by 0.7 hours per decade and were associated with the largest yield losses, reducing county-level yield by up to 7.6% at approximately 10 hours of exposure. County-level yield sensitivity also became increasingly negative during 1981–2018, with estimated changes of −31.5 kg ha^{-1} h^{-1} to −15.6 kg ha^{-1} h^{-1}, particularly during the middle and late reproductive stages. Within the XGBoost models, changes in HDW occurrence were the most influential predictors of sensitivity trends, and field-trial analyses showed consistent temporal patterns. These findings reveal increasing wheat vulnerability to compound atmospheric stress and highlight a growing adaptation gap to intensifying HDWs in China.

Climate warming is intensifying compound extremes that threaten crop production across major agricultural regions. Land–atmosphere coupling can amplify hot–dry extremes by linking soil moisture (SM) loss to reduced evaporative cooling[1]. This feedback has been documented during compound drought–heat events in China, while national analyses show that these events have become stronger and longer[2–4]. Studies of wheat-growing regions further show that plausible heat and drought events can exceed historical records and that compound hot–dry days have increased during Chinese crop-growing seasons[5,6]. Across China's wheat belt, hot–dry–windy events (HDWs) add strong winds to high temperature and low humidity, creating acute stress during heading and grain filling[7,8].

HDWs differ from conventional heat or drought events because they abruptly alter crop microclimates and can reduce yield within hours[7–9]. Previous studies have documented increasing HDW frequency[7,10–12], but national-scale trends, including differences among physiologically distinct wet-to-dry transitions, and their yield effects remain incompletely resolved. This uncertainty is particularly important in China, where wheat is frequently exposed during grain filling[11–13]. Three event types are recognized: high-temperature low-humidity (HTLH), post-rain green-wilt (PRGW) and drought–wind (DTWD). They arise from distinct meteorological sequences, affect different regions and growth stages, and produce different physiological symptoms[7]. Continuous national data linking event-specific exposure to crop phenology and yield, however, have been lacking.

Characterizing exposure alone is insufficient because adaptation can alter the yield response to a given event. Crop–climate studies have established widespread yield risks from extremes[14–17], but many rely on

[1]State Key Laboratory of Soil and Water Conservation and Desertification Control, Institute of Soil and Water Conservation, Northwest A&F University, Yangling, China. [2]College of Agriculture, Shanxi Agricultural University, Taigu, China. [3]NSW Department of Primary Industries, Wagga Wagga Agricultural Institute, Wagga Wagga, New South Wales, Australia. [4]Hawkesbury Institute for the Environment, Western Sydney University, Richmond, New South Wales, Australia. [5]Gulbali Institute for Agriculture, Water and Environment, Charles Sturt University, Wagga Wagga, New South Wales, Australia. [6]College of Horticulture Science, Zhejiang A&F University, Hangzhou, China. [7]Key Laboratory for Agricultural Soil and Water Engineering in Arid Area of Ministry of Education, Northwest A&F University, Yangling, China. [8]Frontier Technology Research Institute of China Agricultural University, Shenzhen, China. ✉e-mail: tongcong_jiang@nwafu.edu.cn; yuq@nwafu.edu.cn; mahaijiao2021@163.com

https://doi.org/10.1038/s43016-026-01452-8

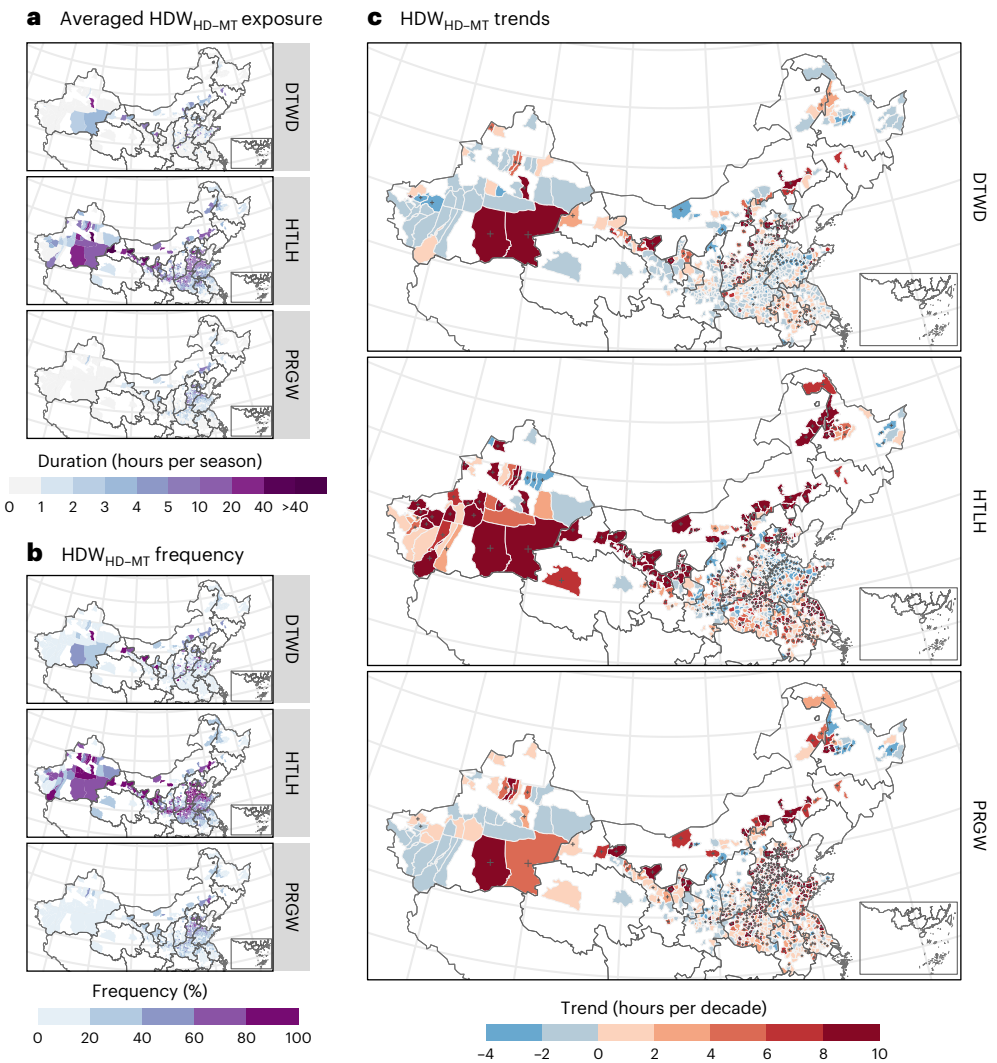


Fig. 1 | Exposure, occurrence frequency and temporal trends of three HDW types across the Chinese wheat belt. a, Mean exposure duration during HD–MT for DTWD, HTLH and PRGW from 1981 to 2018. **b**, Proportion of years in which each HDW type occurred. **c**, County-level trends in annual exposure duration (hours per decade) estimated with Poisson regression. The plus symbols denote $P < 0.05$, with symbol size scaled to county area.

model-defined scenarios that cannot fully represent responses under evolving management[18–22]. China has released thousands of wheat varieties since 2007[23,24], while irrigation and other agronomic measures are used to limit HDW damage[25]. Whether these changes have reduced HDW sensitivity remains unknown. Yield records alone cannot identify the cultivar and management adjustments underlying any observed change in sensitivity. This gap reflects limitations in long-term observations and uncertainty in crop–climate models[26–29]. Quantifying changes in yield sensitivity under observed production conditions is therefore necessary to evaluate adaptation effectiveness[30,31].

Here we assessed how HDW exposure and wheat yield sensitivity changed across China. A random-forest model used 7,413 station–year phenology records (1981–2018) to estimate county-level growth stages, which were combined with hourly reanalysis data to characterize exposure. Yield responses were quantified using 32,318 county-year records (1981–2018) and 6,525 variety-site-year observations from national certification trials (2007–2018). Production-cost data covered fertilization, irrigation, mechanization and seed. Fixed-effects models estimated mean yield responses and temporal changes in sensitivity. XGBoost models evaluated the predictive importance of concurrent trends in HDW exposure and production costs. This framework provides a national assessment of changing wheat vulnerability to HDWs.

Results

Spatial patterns and long-term trends in HDW exposure

HTLH dominated HDW exposure across the Chinese wheat belt. Mean exposure increased sharply from east to west and exceeded 40.0 hours per season in the Hexi Corridor and Xinjiang (Fig. 1a). DTWD and PRGW exposures remained below 5.0 hours per season, although all three event types occurred most frequently in Xinjiang and the Huang-Huai-Hai Plain (Fig. 1a). Across reproductive phases, DTWD exposure remained comparatively stable, whereas PRGW peaked during the middle and late phases (Supplementary Figs. 1 and 2). HTLH also peaked during these phases in the Huang-Huai-Hai Plain but persisted throughout reproduction in Xinjiang, Inner Mongolia and the Hexi Corridor (Supplementary Figs. 1 and 2). HTLH accounted for more than 50% of events across most regions and increased nationally by 0.7 hours per decade (Fig. 1b,c). DTWD and PRGW each occurred in no more than 10.0% of years across most regions (Fig. 1b).

Long-term trends differed markedly among HDW types and regions. DTWD changed little during 1981–2018 (Fig. 1c; −1.0 hours per decade to 1.0 hours per decade). By contrast, HTLH increased significantly by more than 10.0 hours per decade in the Hexi Corridor (Fig. 1c). Significant increases of 1.0–2.0 hours per decade also occurred in parts of Inner Mongolia, Shanxi, Henan and Jiangsu

https://doi.org/10.1038/s43016-026-01452-8

Table 1 | Mean R^2 across 10,000 bootstrap regressions for county-level and national variety-trial yield models

Variables	Model	R^2	
		County-level	Field trial
SM, GDD, FDD, EDD	TSMM	0.613	0.447
SM, GDD, FDD, EDD, HDW	TSDM	0.664	0.476
SM, GDD, FDD, EDD, HDW, Cost	TSCD	0.744	0.572
Precipitation, GDD, FDD, EDD	TPMM	0.602	0.431
Precipitation, GDD, FDD, EDD, HDW	TPDM	0.651	0.466
Precipitation, GDD, FDD, EDD, HDW, Cost	TPCD	0.722	0.563

TSMM and TPMM are baseline models that use SM and precipitation, respectively; TSDM and TPDM add HDW exposure; TSCD and TPCD further add production-cost variables. The six model variants are defined in Methods and Supplementary Texts 2 and 3.

(Fig. 1c). Declines of −4.0 hours per decade to −0.7 hours per decade were confined to the Guanzhong Plain and Shandong–Hebei border (Fig. 1c). PRGW increased locally by up to 1.0 hours per decade in the Huang-Huai-Hai Plain. Stage-specific estimates confirmed increasing HTLH exposure in Xinjiang, the Hexi Corridor and Inner Mongolia, but mixed changes across the Guanzhong and Huang-Huai-Hai Plains (Supplementary Fig. 3).

HDW occurrence shifted earlier with wheat phenology, exposure trends most closely matched low-humidity trends and nearly all field-trial varieties were exposed. During the most recent decade, HDW occurrence advanced by approximately 0–5.0 days alongside wheat phenology, particularly for winter wheat (Supplementary Fig. 4). During heading to maturity (HD–MT), cumulative hours with wind speed (W) ≥ 3.0 m s^{-1} or hourly temperature (T) ≥ 30.0 °C showed mostly non-significant trends. By contrast, hours with relative humidity (RH) ≤ 30% increased significantly by 2.0–5.0 hours per season in Xinjiang, Gansu, Shaanxi, Shanxi and Hebei. The spatial pattern of these low-humidity trends closely matched those of HTLH and PRGW exposure (Supplementary Fig. 5). Field-trial data further indicated that 1.0% of varieties were not exposed to HDWs. Among the 99.0% that were exposed, 84.5% experienced yield anomaly (Supplementary Fig. 6).

Yield responses to HDWs

The six fixed-effects specifications separated the contributions of HDW exposure and production-cost variables to model performance (Table 1). Full coefficient estimates in standardized and original units are provided in Supplementary Tables 2–13. Adding HDW exposure increased R^2 by 3.0–5.0 percentage points relative to the corresponding baseline models (Table 1). Adding production-cost variables resulted in an additional increase of 7.0–10.0 percentage points (Table 1). Yield responses to both SM and precipitation varied nonlinearly among growth stages (Fig. 2a,b). In the SM-based models, yield was comparatively insensitive to SM variation from planting to jointing (Fig. 2a). In the precipitation-based model, rainfall effects were weaker during HD–MT, whereas very high precipitation was associated with lower yields (Fig. 2b).

Among the three HDW types, HTLH showed the largest estimated adverse yield response (Fig. 2c). A 1-s.d. increase in exposure corresponded to yield reductions of 5.3–7.6% in county data and 0.4–12.7% in variety-trial data. Analyses of county-level and field data showed that most models initially identified the middle HD–MT stage as the period most vulnerable to HTLH (Supplementary Fig. 7). After including cost variables, however, this stage was no longer identified as the most vulnerable. County data indicated that the impacts of PRGW peaked during the late HD–MT stage, whereas field data showed a peak in the middle HD–MT stage (Supplementary Fig. 7). Furthermore, county-level data suggested that HTLH and PRGW had a more pronounced impact on yields than extreme degree days (EDD) and freezing degree days (FDD), with corresponding effects of −3.6% to −0.9% and −1.3% to 0.2% per standardized unit, respectively (Supplementary Fig. 8). Spatially, regions such as Inner Mongolia, Xinjiang, Beijing, Hebei, Jiangsu, Shaanxi and Henan exhibited yield sensitivities to HTLH that exceeded the national average (Fig. 2d). Moreover, yield sensitivities to PRGW were also higher than the national average in Beijing, Hebei, Jiangsu and Shaanxi (Fig. 2d).

Spatial patterns of estimated yield losses associated with HDWs

By combining the average duration of HDW exposure with yield-response estimates in their original units (Supplementary Tables 9, 10, 12 and 13), we quantified spatial patterns of estimated yield losses associated with HDWs. Spatially, estimated yield losses associated with HTLH during 1981–2018 occurred over a broader area than those associated with DTWD and PRGW, with especially pronounced impacts in the Huang-Huai-Hai Plain, where losses ranged from −400.0 kg ha^{-1} per season to −100.0 kg ha^{-1} per season (Fig. 3). In Xinjiang and Gansu, estimated yield losses associated with HTLH exceeded 500.0 kg ha^{-1} per season (Fig. 3). Specifically, the model estimated that yield losses associated with DTWD were minimal across the study region (−40.0 kg ha^{-1} per season to −10.0 kg ha^{-1} per season). After accounting for production-cost effects, regressions revealed substantial estimated yield losses associated with PRGW in the Huang-Huai-Hai Plain, with estimated reductions ranging from −100.0 kg ha^{-1} per season to −10.0 kg ha^{-1} per season.

Temporal changes in yield sensitivity to HDWs

To quantify temporal changes in the yield impacts of HDWs, we used four fixed-effects models to estimate changes in wheat yield sensitivity to HDWs (equation (5)) using both county-level and field-trial datasets. In the county-level analysis, all models indicated that the negative effect of HTLH on wheat yield strengthened over time, with estimated changes ranging from −31.5 kg ha^{-1} h^{-1} to −15.6 kg ha^{-1} h^{-1} during 1981–2018 (Fig. 4a). By contrast, all models, except the TPCD model, suggested a shift towards positive yield effects of PRGW, with estimated changes in sensitivity ranging from 4.0 kg ha^{-1} h^{-1} to 30.9 kg ha^{-1} h^{-1} (Fig. 4a). For conventional temperature indices, however, temporal changes in sensitivity depended on growth stage and dataset. Across the four county-level models, EDD sensitivity tended to become more adverse from jointing to heading but consistently became less adverse from heading to maturity. Changes in FDD sensitivity from planting to jointing were close to zero (Supplementary Fig. 9).

Changes in yield sensitivity showed substantial spatial heterogeneity across provinces and HDW types. For HTLH, most provinces in northern, northwestern and northeastern China exhibited increasingly negative yield sensitivities, mainly ranging from −40.0 kg ha^{-1} h^{-1} to −10.0 kg ha^{-1} h^{-1} (Fig. 4b). The strongest negative shifts occurred in Gansu, Ningxia, Hebei, Inner Mongolia, Jilin and Jiangsu, where changes approached −40.0 kg ha^{-1} h^{-1} (Fig. 4b). The spatial pattern for PRGW differed markedly. Positive changes, ranging from 10.0 kg ha^{-1} h^{-1} to 40.0 kg ha^{-1} h^{-1}, were concentrated in Shaanxi, Shanxi and Shandong, whereas slight negative changes, ranging from −20.0 kg ha^{-1} h^{-1} to −10.0 kg ha^{-1} h^{-1}, were confined to Hebei, Henan, Jilin and Jiangsu (Fig. 4b).

Although the field-trial records covered a shorter period, they yielded broadly consistent evidence. All models, except the TPCD model, estimated strengthening negative effects of HTLH on yield, comparable to those inferred from the county-level data, with changes of −33.0 kg ha^{-1} h^{-1} to −13.7 kg ha^{-1} h^{-1} during 2007–2018 (Supplementary Fig. 10a). The analysis across breeding cohorts further showed that the negative yield effect of HTLH intensified, rather than weakened, with the release of newer wheat varieties (Supplementary Fig. 10b). By contrast, yield sensitivity to PRGW shifted from negative to positive with the release of newer varieties, suggesting that varietal improvement may have partly offset the adverse effects of PRGW on wheat yield (Supplementary Fig. 10b).

https://doi.org/10.1038/s43016-026-01452-8

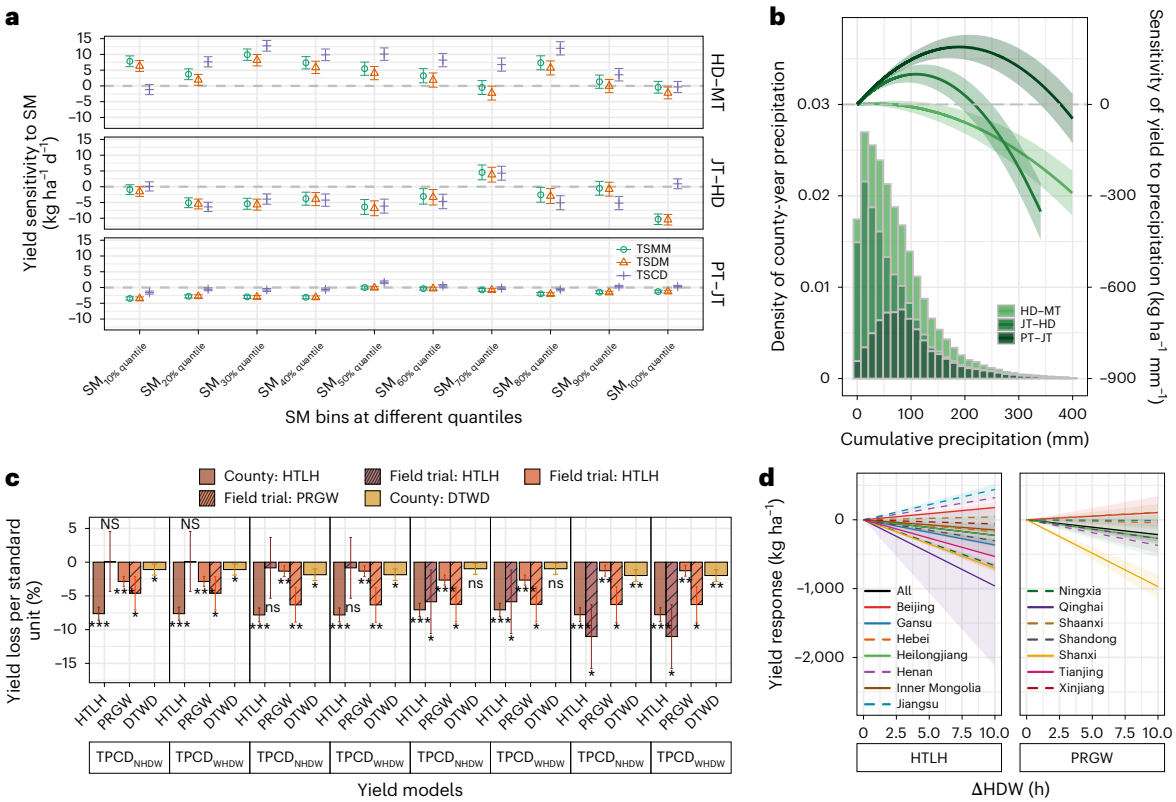


Fig. 2 | Wheat yield responses to water-supply indicators and HDWs in county and national variety-trial datasets. a, Yield sensitivity across growth stages and ten SM percentile bins estimated with the SM-based models TSMM (baseline climate variables), TSDM (TSMM plus HDW exposure) and TSCD (TSDM plus production costs). Points and error bars show bootstrap means and 95% confidence intervals from 10,000 regressions. PT–JT, JT–HD and HD–MT denote planting-to-jointing, jointing-to-heading and heading-to-maturity stages, respectively. **b**, Nonlinear yield response to cumulative precipitation by growth stage in the precipitation-based baseline model (TPMM); the line and shading show the bootstrap mean and 95% confidence interval. **c**, Standardized yield responses to DTWD, HTLH and PRGW estimated with SM-based models (TSDM and TSCD) and precipitation-based models (TPDM and TPCD). Hatched and solid bars denote variety-trial and county-level estimates, respectively. NHDW and WHDW indicate whether high-temperature hours coinciding with HDWs were excluded from (no HDW) or retained (with HDW) in the EDD index. One standard deviation of DTWD, HTLH and PRGW exposure was 3.6h , 10.2h and 3.1 h, respectively, at the county scale and 10.3 h and 5.7 h for HTLH and PRGW, respectively, in the variety trials. For **c**, bars show mean coefficient estimates and error bars indicate ±1 s.d. across 10,000 bootstrap fixed-effects regressions per coefficient; these regressions are bootstrap resamples rather than independent observations. For each regression, two-sided *P* values for individual coefficients were obtained from the coefficient *t*-tests returned by the feols function in the fixest R package. NS, $P \geq 0.05$, $^{*}P < 0.05$, $^{**}P < 0.01$, $^{***}P < 0.001$. The units of analysis were county-year and variety-site-year records; the full datasets comprised $n = 32{,}318$ county-year observations and $n = 6{,}525$ variety-site-year observations. **d**, National and province-specific yield sensitivities to HDW exposure estimated from county data using the TSCD model; lines show estimated yield change along the HDW exposure gradient; the line and shading show the bootstrap mean and 95% confidence interval.

Predictors of temporal changes in yield sensitivity

Using the XGBoost machine-learning framework, we further related temporal trends in wheat yield sensitivity to HDWs, estimated as TSCD-derived $\beta_{\mathrm{HDW\times year}}$, to concurrent shifts in HDW exposure hours and wheat production costs. At the county level, XGBoost identified trends in HTLH exposure as the most influential predictors of yield sensitivity trends during the middle and late HD–MT stages, with relative importance values of 77.5% and 40.8%, respectively (Fig. 5a). Partial-dependence analysis further showed that stronger increases in HTLH exposure were associated with more negative $\beta_{\mathrm{HDW\times year}}$ values during the middle and late HD–MT stages (Fig. 5b).

Field-trial analyses corroborated these patterns. Trends in HTLH exposure were among the most influential predictors during the middle HD–MT stage, with a relative importance of 53.0% (Supplementary Fig. 12a). Partial-dependence results similarly showed that rising HTLH exposure trends were associated with stronger negative $\beta_{\mathrm{HDW\times year}}$ responses during this stage (Supplementary Fig. 12b). Trends in the four major production costs showed stage-dependent effects and, in some cases, increasing cost trends were associated with more negative $\beta_{\mathrm{HDW\times year}}$ values (Supplementary Fig. 14). Thus, higher production-cost trends were not consistently associated with reduced yield sensitivity to HTLH. By contrast, production-cost trends were more important for explaining variation in $\beta_{\mathrm{HDW\times year}}$ for PRGW (Supplementary Fig. 12a). Partial-dependence analysis further indicated that increasing production-cost trends were associated with more positive $\beta_{\mathrm{HDW\times year}}$ values for PRGW (Supplementary Fig. 14).

Discussion

By integrating phenology, reanalysis climate data, county yields, production costs and national variety trials, this study resolves two dimensions of changing HDW risk—exposure and yield sensitivity. HDW exposure changed unevenly across the Chinese wheat belt. Increases were concentrated in Xinjiang, the Hexi Corridor and parts of Inner Mongolia, Shanxi, Henan and Jiangsu. Changes across the Huang-Huai-Hai Plain were generally modest, whereas declines occurred in the Guanzhong Plain and along the Shandong–Hebei border (Fig. 1c). These regional patterns are consistent with earlier assessments[11,12,32,33].

The regional contrast in HDW exposure appears to reflect changes in atmospheric humidity more strongly than changes in wind speed. Hours with $W \geq 3$ m s^{-1} followed a spatial pattern distinct from HDW

https://doi.org/10.1038/s43016-026-01452-8

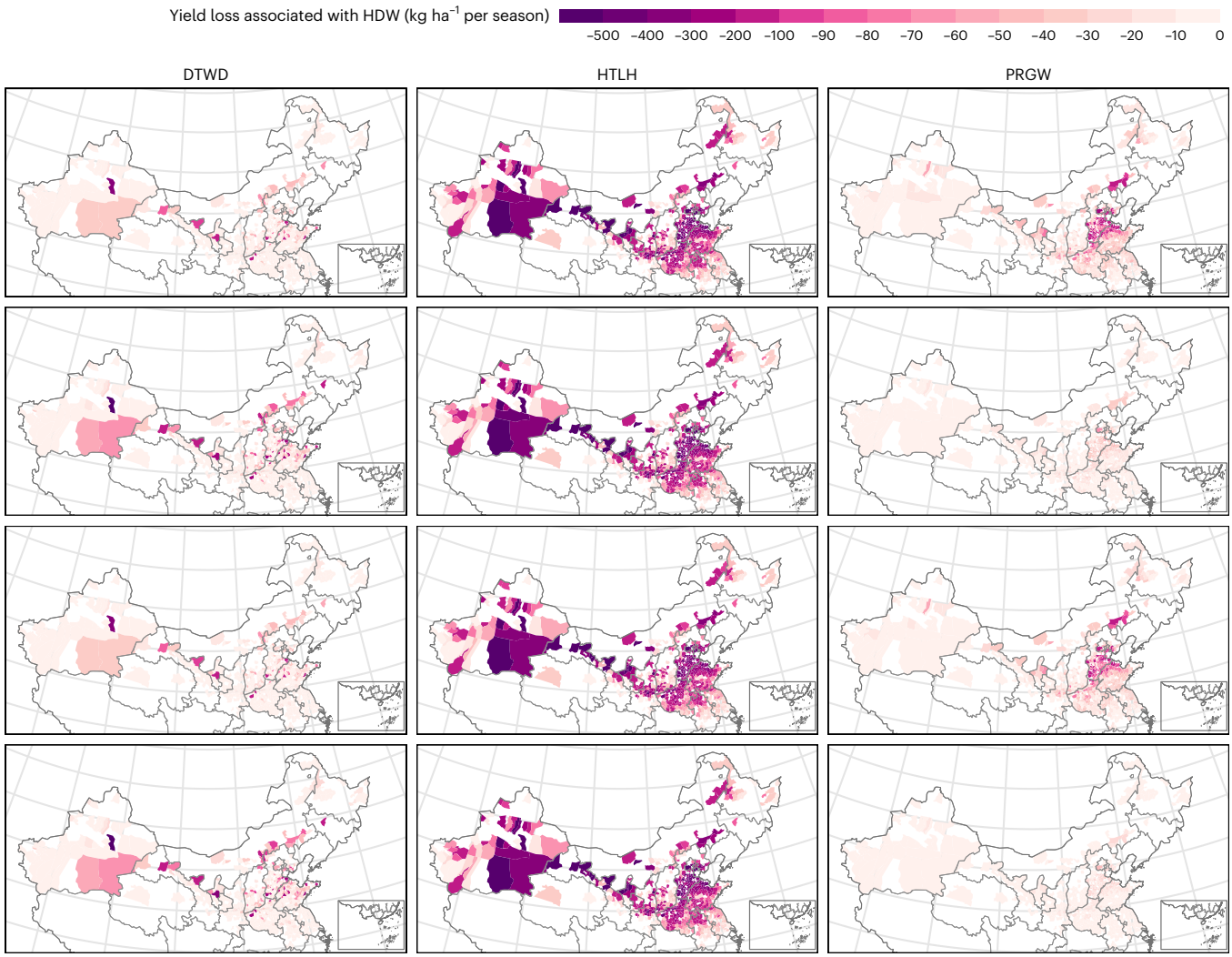


Fig. 3 | Spatial distribution of average estimated wheat yield losses associated with three types of HDW. Columns show DTWD, HTLH and PRGW, and rows represent four alternative fixed-effects models: SM-based models (TSDM and TSCD) and precipitation-based models (TPDM and TPCD). TSDM and TPDM include climate variables and HDW exposure; TSCD and TPCD additionally include production-cost variables. Maps show county-level average estimated yield losses (kg ha^{-1} per season) during 1981–2018, estimated as the product of mean HDW exposure duration and the corresponding county-level yield sensitivity.

trends. This divergence is compatible with reported global stilling over China[34,35] and the subsequent stabilization or partial recovery of winds, particularly in northwestern China[36,37]. By contrast, increases in hours with RH ≤ 30% closely matched the spatial distribution of increasing HDW exposure. Asymmetric changes in humidity, temperature and wind may therefore explain the stronger trends in northwestern China and Inner Mongolia. Phenological change may have further modified exposure. Earlier crop development coincided with earlier HDW occurrence (Supplementary Fig. 4), potentially shifting exposure windows within sensitive reproductive stages. Most cultivars in the national trials nevertheless remained exposed during reproduction (Supplementary Fig. 6), indicating limited phenological escape under the tested breeding and management conditions.

Wheat in China also showed greater HDW sensitivity than the 4% yield loss (91 kg ha^{-1} per 10 h) estimated for US winter wheat in ref. 8. This contrast may reflect lower event thresholds, more frequent exposure, cultivar differences, irrigation infrastructure and management[38]. The estimated sensitivity is consistent with controlled Chinese field experiments, which reported a 6–8% reduction in grain weight after 4 h of HDW exposure[39]. Our results further show that yield responses depend on event type, wet-to-dry transition and timing. HTLH, PRGW and DTWD represent distinct combinations of temperature, atmospheric aridity, antecedent moisture and wind. Their effects also varied among reproductive phases and provinces. Process-based crop models could therefore benefit from representing sub-daily compound stress and stage-dependent physiological responses explicitly.

Most previous assessments quantified crop responses to climate extremes without directly examining how sensitivity covaried with management over time[40–44]. In our analysis, HTLH sensitivity became more negative even as measured production inputs increased. The contrasting temporal responses across stress types and growth stages are consistent with uneven adaptation to these stresses. Many agronomic improvements alleviate soil-water or nutrient limitations, whereas HTLH imposes acute atmospheric demand through concurrent heat, low humidity and wind. Irrigation can reduce soil-water deficits but cannot fully eliminate this evaporative demand[7]. HTLH occurs mainly from heading through mid-to-late grain filling, it may damage leaves and roots during yield formation, shorten effective grain filling and limit post-stress recovery. As management and genetic resistance reduce other yield limitations[24,45,46], HDWs may explain a larger share of the remaining yield variability. Together, these patterns are consistent with this interpretation. County and variety-trial analyses differed in

https://doi.org/10.1038/s43016-026-01452-8

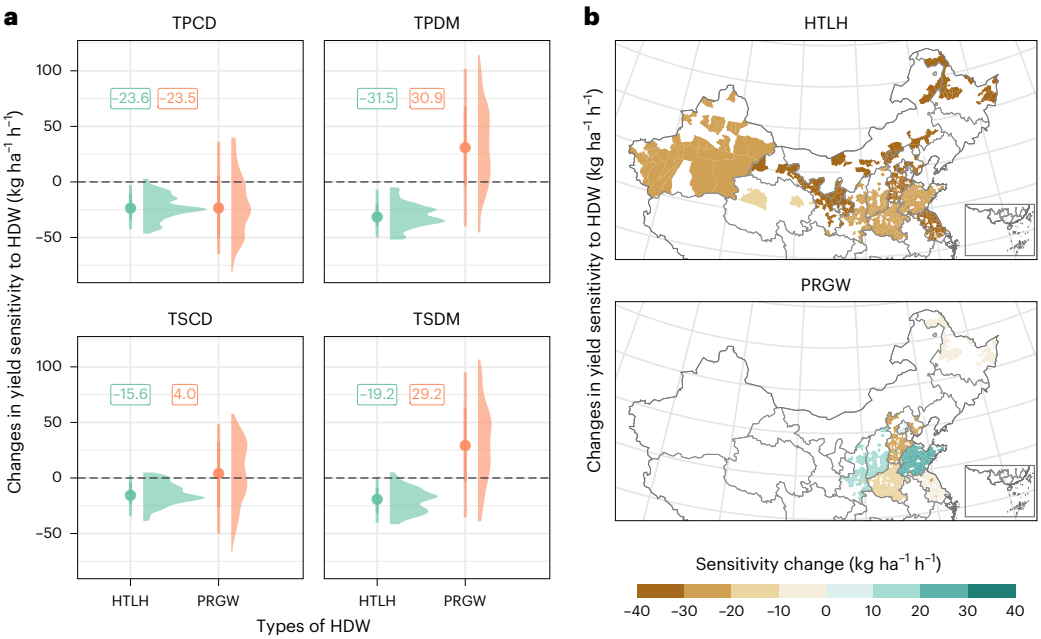


Fig. 4 | Temporal changes in wheat yield sensitivity to HDWs. a, Changes in sensitivity to HTLH and PRGW estimated from county-level data (1981–2018) using four fixed-effects models: SM-based TSDM and TSCD, and precipitation-based TPDM and TPCD. Ridge plots show distributions of 10,000 bootstrap estimates, with points and error bars indicating means and 95% confidence intervals. The boxed numbers in **a** indicate the median values. Negative values denote an increasingly adverse yield response over time; positive values denote a shift towards less negative or more positive responses. The changes in wheat yield sensitivity to HDW during three phases from heading to maturity estimated by four fixed-effects models are shown in Supplementary Fig. 11. **b**, Province-specific changes in sensitivity to HTLH and PRGW between 1981 and 2018 estimated with the TSCD model. Map values are means of 10,000 bootstrap estimates and represent the change in sensitivity (kg ha^{-1} h^{-1}) between 1981 and 2018.

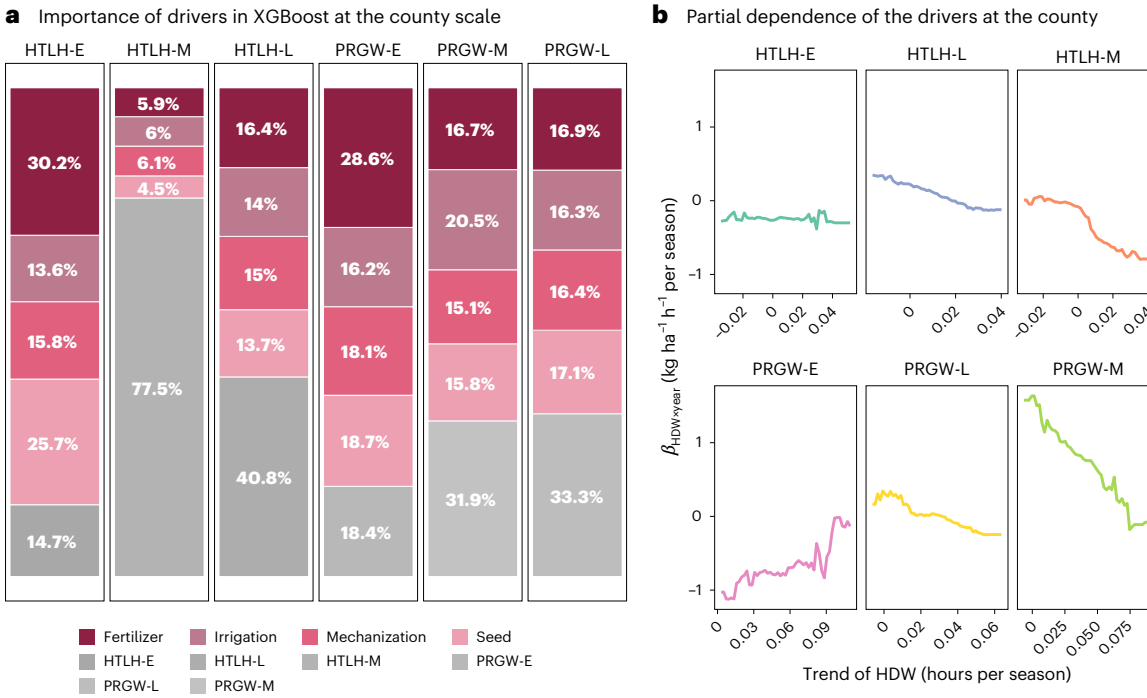


Fig. 5 | Predictive importance of HDW and production-cost trends for estimated changes in wheat yield sensitivity. a, Relative importance of trends in HDW exposure and four production-cost categories in XGBoost models predicting the fixed-effects HDW-by-year coefficients. **b**, Partial dependence of HDW-by-year coefficients ($\beta_{HDW\times year}$) on HDW exposure trends. E, M and L denote the early, middle and late thirds of HD–MT. Model R^2 ranged from 0.34 to 0.71 across stages and HDW types (Supplementary Fig. 13).

magnitude but showed similar temporal directions across contrasting management and environmental conditions.

Evidence from other crop systems places these results within a broader shift in climate sensitivity. Declining winds initially benefited Chinese maize yields, but this effect weakened as winds recovered[47]. In the US Corn Belt, maize sensitivity to SM deficits has increased by approximately 55% since 1999[30]. Together with evidence for US winter wheat[8], these findings indicate that climate sensitivity can increase

despite continued breeding and agronomic investment. Adaptation strategies must therefore address sub-daily compound atmospheric stress alongside conventional heat, drought and soil-water constraints. Relevant responses include phenology-informed warning systems, targeted irrigation timing and cultivar screening for tolerance to compound stress.

Although we integrated multiple data sources to assess the effects of HDWs on wheat yields in China, several limitations remain. First, the climatic variables used to identify HDWs were obtained from multiple reanalysis products. Differences in data assimilation, model formulation, input observations and spatiotemporal resolution may affect estimates of HDW frequency and long-term trends. The magnitude of inferred long-term changes therefore remains sensitive to the reanalysis dataset used. Second, because HDWs are highly localized, county-level meteorological averages may not fully resolve field-scale exposure. Temporal trends estimated from county-level data may also combine the effects of climate variability, breeding progress, irrigation and wider agricultural modernization. These overlapping influences are difficult to disentangle fully from observational data alone. Third, although bias-corrected provincial irrigation-cost data were incorporated, consistently documented high-resolution irrigation information was unavailable. This limitation constrained our ability to separate irrigated from rainfed systems and to quantify the mitigation potential of supplemental irrigation. Finally, variety release year denotes breeding cohorts rather than genetic gain. Variety-trial trends therefore reflect average cohort performance across the sampled environments and management regimes. Future work should attribute changes in HDW occurrence and intensity to climatic and environmental drivers more explicitly, and separate the combined effects of breeding progress, management and environmental change on crop vulnerability to HDWs.

Methods

Data sources

County-level wheat yields were compiled from statistical yearbooks for 1981–2018, yielding 32,318 county-year records[48] (Supplementary Fig. 15). Phenological observations for sowing, jointing, heading and maturity were obtained from China Meteorological Administration agricultural meteorological stations, comprising 7,413 station–year records (Supplementary Figs. 16 and 17). These observations were used to estimate county-level phenology as described below.

Hourly 2-m air temperature was obtained from ERA5-Land, 10-m wind speed from the reconstruction of near-surface hourly wind speed datasets[49] and 2-m relative humidity from the China Meteorological Forcing Dataset[50,51]. The original 3-hourly relative humidity series was interpolated to hourly resolution with a spline. Temperature and wind products were evaluated against hourly observations from 92 stations (Supplementary Figs. 18 and 19). Relative humidity was evaluated against daily station observations because long-term hourly records were unavailable (Supplementary Figs. 20–22). Daily precipitation was obtained from the China Meteorological Forcing Dataset.

Two complementary 0–20-cm SM products covered 1981–1992[52] and 1993–2018[53], providing a continuous record over the study period. Provincial wheat production costs for 1981–2018 were obtained from the Cost-Benefit Data of Agricultural Products in China[54]. Missing years were interpolated from temporal trends (Supplementary Fig. 23). The datasets provide detailed information on production costs (fertilization, irrigation, mechanization and seed) for major crops[55] and were adjusted to county and field scale (Supplementary Text 1).

National wheat variety certification trials

We used 6,525 variety-site-year observations from 460 cultivars evaluated at 77 sites during 2007–2018 (Supplementary Figs. 24 and 25). The trials were conducted across China's ten wheat agroecological zones as part of the National Crop Variety Certification Committee evaluation process (Supplementary Text 3). Preliminary, regional and production trials progressively evaluated yield potential, adaptation, stress resistance and quality. Records included sowing, jointing, heading and maturity dates and grain yield. Cultivars were grouped by release year to represent successive breeding cohorts, and their mean HDW sensitivity was estimated across the environments represented in the trials.

County-level phenology estimation

County-level phenological dates were estimated with province-specific random-forest models fitted to station observations. For each province and growth stage, the earliest and latest observed dates defined the prediction window. Stage-specific mean temperature and cumulative precipitation within each window, together with latitude, longitude and year, were used as predictors. Separate models were fitted for sowing, jointing, heading and maturity (Supplementary Fig. 26) and applied to estimate county-level dates (Supplementary Figs. 27 and 28).

Climate variables

Growing degree days (GDD), EDD and FDD were calculated with growth-stage-specific thresholds for winter and spring wheat (equations (1)–(3)). Hours classified as HDWs were excluded from EDD to reduce overlap between the exposure metrics.

$$\mathrm{GDD}=\sum_{d=1}^{d=n}\sum_{h=1}^{h=24}\mathrm{GDD}_h^d;\ \mathrm{GDD}_h=\begin{cases}0 & T_h<T_{\mathrm{base}}\\ \frac{(T_h-T_{\mathrm{base}})}{24} & T_{\mathrm{base}}\le T_h\le T_{\mathrm{opt}}\\ \frac{T_{\mathrm{opt}}-T_{\mathrm{base}}}{24} & T_h>T_{\mathrm{opt}}\end{cases} \quad (1)$$

$$\mathrm{EDD}=\sum_{d=1}^{d=n}\sum_{h=1}^{h=24}\mathrm{EDD}_h^d;\ \mathrm{EDD}_h=\begin{cases}0 & T_h\le T_{\mathrm{opt}}\\ \frac{T_h-T_{\mathrm{opt}}}{24} & T_h>T_{\mathrm{opt}}\end{cases} \quad (2)$$

$$\mathrm{FDD}=\sum_{d=1}^{d=n}\sum_{h=1}^{h=24}\mathrm{FDD}_h^d;\ \mathrm{FDD}_h=\begin{cases}\frac{T_h-T_{\mathrm{frez}}}{24} & T_h\le T_{\mathrm{frez}}\\ 0 & T_h>T_{\mathrm{frez}}\end{cases} \quad (3)$$

Here, d denotes days, h denotes hours within each day (h = 1–24) and n is the total number of days in the calculation period; T_{frez}, T_{base} and T_{opt} denote the growth-stage-specific freezing, base and optimum temperature thresholds, respectively.

Definition of HDWs

HDWs were identified from Chinese meteorological standards and classified as HTLH, PRGW or DTWD. Classification used hourly temperature (T), relative humidity (RH) and wind speed (W), together with antecedent rainfall and, in specified regions, relative soil humidity. Operational thresholds are summarized below. Supplementary Figs. 29 and 30 summarize damage pathways and inter-event correlations, respectively.

HTLH events

HTLH was defined from heading to maturity by RH ≤ 30% and $W \ge 3$ m s^{-1}, with temperature thresholds specified by region and SM. In North China, the Huang-Huai-Hai and Guanzhong Plains, the threshold was 31 °C when 20-cm soil humidity was ≤60%, and 33 °C otherwise. A threshold of 32 °C was used for winter wheat in Xinjiang and spring wheat in the Hetao, Ningxia and Hexi Corridor regions. Field diagnosis was based on dried or split awn tips, leaf rolling and wilting, bleached spikes and premature leaf senescence.

PRGW events

PRGW was defined from heading to maturity when $T \ge 30$ °C, RH ≤ 40% and $W \ge 3$ m s^{-1} occurred within 3 days after rainfall >5 mm. Events also required a V-shaped temperature sequence, with temperature falling to ≤20 °C after rainfall and then rebounding sharply. Field diagnosis was based on green but wilted spikes, prematurely dried upper

spikelets, brittle awns, tightly closed glumes, detached grains and a dark-green peduncle.

DTWD events

DTWD was defined mainly from heading to maturity in Xinjiang and the Loess Plateau. Events were identified when $T \geq 25$ °C, RH ≤ 30% and $W \geq 15$ m s^{-1}. This definition reflects the strong atmospheric drying imposed by high wind speed, which can damage wheat at lower temperatures than HTLH. Field symptoms included severely rolled or twisted leaves, torn leaf margins, dry brittle awns, shortened ripening and partially filled or shrivelled grains.

Spatiotemporal patterns of HDW exposure

The HD–MT period was divided into equal early, middle and late thirds. County-level trends in annual exposure hours were estimated by Poisson regression for each HDW type. The occurrence frequency was calculated as the proportion of years with at least one event during 1981–2018.

Yield sensitivity to HDWs

We estimated wheat yield sensitivity to the three HDW types in both county-level and variety-trial datasets using a generalized fixed-effects framework (equation (4)). To test the robustness of these estimates, we implemented six specifications that shared the same model structure but varied in the water-supply covariate and the inclusion of HDW exposure and production-cost covariates. Water supply was included because HDW effects may vary with crop water conditions; it was represented by SM deciles or, in parallel specifications, by stage-specific precipitation. Production costs were included to account for observed changes in input intensity, including irrigation expenditure, that could confound estimated HDW responses (Table 1).

$$Y_{i,t} = W_{i,t}^{\top}\boldsymbol{\beta}_W + T_{i,t}^{\top}\boldsymbol{\beta}_T + d_H H_{i,t}^{\top}\boldsymbol{\beta}_H + d_C C_{i,t}^{\top}\boldsymbol{\beta}_C + \mu_i + \lambda_t + \varepsilon_{i,t} \quad (4)$$

In equation (4), i indexes counties and t indexes years; $\mathbf{X}_{i,t}^{\top}\boldsymbol{\beta}_X$ represents the inner product of a covariate vector and its corresponding coefficient vector. $W_{i,t}$ denotes water-supply covariates, specified as accumulated days in SM bins or stage-specific precipitation; $T_{i,t}$ contains stage-specific GDD, FDD and EDD; $H_{i,t}$ contains HTLH, PRGW and DTWD exposure during the early, middle and late thirds of HD–MT; and $C_{i,t}$ contains fertilization, irrigation, mechanization and seed costs. Superscript \(\top\) denotes vector transposition. The vectors β_W, β_T, β_H and β_C contain the coefficients for the water-supply, temperature-related, HDW-exposure and production-cost covariates, respectively. The indicators d_H and d_C determine whether HDW and production-cost blocks are included, whereas μ_i and λ_t represent county and year fixed effects. The residual $\varepsilon_{i,t}$ captures unexplained variation.

TSMM, TSDM and TSCD are SM-based specifications without HDW, with HDW and with both HDW and production costs, respectively. TPMM, TPDM and TPCD are the corresponding precipitation-based specifications (Table 1). Expanded county models are provided in Supplementary Text 2, and variety-trial models are provided in Supplementary Text 3.

The two SM products differed in their statistical distributions and were therefore converted independently to county-specific deciles. For each growth stage, cumulative days in each decile were used to estimate SM responses. This harmonization avoided treating absolute SM values from the two products as directly equivalent. Decile bins were defined at 10% intervals from 0 to 100%.

Yield and explanatory variables were standardized as z scores to compare responses across climate indices and HDW types. Estimates in standardized and original units are reported in Supplementary Tables 2–13.

Temporal changes in yield sensitivity

Year-by-year panel regressions may not fully account for common time effects or spatial autocorrelation across counties[31]. We therefore extended the TSDM, TSCD, TPDM and TPCD specifications by interacting calendar year with selected climate exposures (equation (5)). Uncertainty was quantified with 10,000 bootstrap replications. Multicollinearity among HDW, temperature, soil and cost variables was evaluated in every bootstrap fit with the feols function in the fixest R package.

$$Y_{i,t} = \left(X_{i,t}^{(m)}\right)^{\top}\beta^{(m)} + \tilde{t}\,Z_{i,t}^{\top}\gamma^{(m)} + \mu_i + \lambda_t + \varepsilon_{i,t}. \quad (5)$$

In equation (5), $X_{i,t}$ contains the main-effect covariates of specification model m, and $Z_{i,t}$ contains FDD during planting to jointing, EDD during jointing to heading and HD–MT, and HTLH and PRGW exposure during each of the three HD–MT phases. Calendar year $\tilde{t}$ was centred at the first year of the corresponding dataset; the coefficients in $\gamma^{(m)}$ therefore represent annual changes in yield sensitivity. DTWD was excluded because of its low occurrence frequency. Year was centred at the start of the panel before constructing the interaction terms so that HDW-by-year coefficients represent annual changes in yield sensitivity relative to the initial year.

Expanded county and variety-trial formulations are provided in Supplementary Texts 4 and 5. Uncertainty for the field-trial models was quantified with the hierarchical procedure described in Supplementary Text 6. Regional mean sensitivities and province-specific temporal changes were estimated with interaction models described in Supplementary Texts 7 and 8. Model estimation and multicollinearity diagnostics are detailed in Supplementary Text 9.

Predictors of temporal changes in yield sensitivity

XGBoost models evaluated the relative predictive contributions of trends in HDW exposure and four production-cost categories to bootstrap estimates of HDW-by-year coefficients. Each coefficient was paired with the corresponding mean predictor trends. Relative importance and partial-dependence values were interpreted as associations within the fitted models. Models were fitted with the xgboost package, and partial-dependence profiles were calculated with the pdp package in R.

Reporting summary

Further information on research design is available in the Nature Portfolio Reporting Summary linked to this article.

Data availability

Publicly available environmental data were obtained from the following repositories: ERA5-Land hourly 2-m air temperature from the Copernicus Climate Data Store at (https://doi.org/10.24381/cds.e2161bac); reconstructed hourly 10-m wind speed for China from Zenodo at https://doi.org/10.5281/zenodo.8350860 (ref. 56); 3-hourly relative humidity and daily precipitation from the China Meteorological Forcing Dataset v2.0 at the National Tibetan Plateau/Third Pole Environment Data Center (https://doi.org/10.11888/Atmos.tpdc.302088); SMML-CHN v1.0 soil moisture from the NASA Aura Validation Data Center (https://avdc.gsfc.nasa.gov/pub/data/project/SMML_CHN/); and the wheat 0–20-cm daily soil moisture from Zenodo at https://doi.org/10.5281/zenodo.6834530 (ref. 57) and https://doi.org/10.5281/zenodo.6822591 (ref. 58). County-level wheat yield records were compiled from national and provincial statistical yearbooks published by the National Bureau of Statistics of China and available at https://www.stats.gov.cn/sj/ndsj/. Crop-phenology observations were obtained from the China Meteorological Administration Data Service Centre (https://data.cma.cn/). Provincial wheat production-cost records were compiled from annual editions of the National Compilation of Cost-Benefit Data of Agricultural Products published by the National

Development and Reform Commission and China Statistics Press. Provincial wheat production-cost records are available via figshare at https://doi.org/10.6084/m9.figshare.33653194 (ref. 59). National wheat variety-trial records were obtained from annual national wheat variety regional trial reports compiled by the National Agricultural Technology Extension and Service Center and available at https://www.natesc.org.cn/. Source data are provided with this paper.

Code availability

Custom R scripts for climate data evaluation, county-level phenology estimation, HDW exposure assessment, yield-sensitivity analysis and attribution are available at https://github.com/Jhone-FML/Crop-yield-loss-at-HDW. R scripts for figures are available via figshare at https://doi.org/10.6084/m9.figshare.33653194 (ref. 59).

References

1. Seneviratne, S. I., Lüthi, D., Litschi, M. & Schär, C. Land–atmosphere coupling and climate change in Europe. *Nature* **443**, 205–209 (2006).
2. Fu, K. & Wang, K. Contributions of local land-atmosphere coupling and mesoscale atmospheric circulation to the 2013 extreme flash drought and heatwave compound event over Southwest China. *J. Geophys. Res. Atmos.* **128**, e2023JD039406 (2023).
3. Wen, Z., Yu, R., Zhai, P., Yin, Y. & Li, L. Z. The evolution process of a prolonged compound drought and hot extreme event in Southwest China during the 2019 pre-monsoon season. *Atmos. Res.* **283**, 106551 (2023).
4. Fu, K. et al. Flash drought and heatwave compound events increased in strength and length from 1980 to 2022 in China. *Weather Clim. Extrem.* **46**, 100720 (2024).
5. Coughlan de Perez, E., Ganapathi, H., Masukwedza, G. I., Griffin, T. & Kelder, T. Potential for surprising heat and drought events in wheat-producing regions of USA and China. *npj Clim. Atmos. Sci.* **6**, 56 (2023).
6. Lu, Y., Hu, H., Li, C. & Tian, F. Increasing compound events of extreme hot and dry days during growing seasons of wheat and maize in China. *Sci. Rep.* **8**, 16700 (2018).
7. Huo, Z. et al. Review on disaster of hot dry wind for wheat in China [in Chinese]. *J. Appl. Meteorol. Sci.* **30**, 129–141 (2019).
8. Zhao, H. et al. US winter wheat yield loss attributed to compound hot–dry–windy events. *Nat. Commun.* **13**, 7233 (2022).
9. Zhang, Z., Cheng, L., Li, S., Peng, J. & Fan, W. Dry–hot wind effects on physiology of winter wheat. *Chin. J. Ecol.* **34**, 712 (2015).
10. Feng, Y. & Sun, F. Changes in the severity of compound hot–dry–windy events over global land areas. *Ecol. Indic.* **165**, 112207 (2024).
11. Liu, D., Sun, L. & Ni, H. Characteristics of dry–hot–wind in Gansu province and its response to climate change. *J. Glaciol. Geocryol.* **30**, 81–86 (2008).
12. Yang, F., Zhu, Y. & Liu, W. Occurrence rules and risk zoning of dry–hot wind in winter wheat producing areas of North China [in Chinese]. *J. Nat. Disasters* **22**, 112–121 (2013).
13. Li, S. et al. A comprehensive index for assessing regional dry–hot wind events in Huang-Huai-Hai region. *China Phys. Chem. Earth* **116**, 102860 (2020).
14. Lesk, C. et al. Stronger temperature–moisture couplings exacerbate the impact of climate warming on global crop yields. *Nat. Food* **2**, 683–691 (2021).
15. Rigden, A., Mueller, N. V., Holbrook, N., Pillai, N. & Huybers, P. Combined influence of soil moisture and atmospheric evaporative demand is important for accurately predicting US maize yields. *Nat. Food* **1**, 127–133 (2020).
16. Zhao, C. et al. Temperature increase reduces global yields of major crops in four independent estimates. *Proc. Natl Acad. Sci. USA* **114**, 9326–9331 (2017).
17. Agnolucci, P. et al. Impacts of rising temperatures and farm management practices on global yields of 18 crops. *Nat. Food* **1**, 562–571 (2020).
18. Singh, P. et al. Quantifying potential benefits of drought and heat tolerance in rainy season sorghum for adapting to climate change. *Agric. For. Meteorol.* **185**, 37–48 (2014).
19. Minoli, S., Jägermeyr, J., Asseng, S., Urfels, A. & Müller, C. Global crop yields can be lifted by timely adaptation of growing periods to climate change. *Nat. Commun.* **13**, 7079 (2022).
20. Jiang, T. et al. Prioritizing agronomic practices and uncertainty assessment under climate change for winter wheat in the Loess Plateau. *China Agric. Syst.* **212**, 103770 (2023).
21. Elliott, J. et al. Constraints and potentials of future irrigation water availability on agricultural production under climate change. *Proc. Natl Acad. Sci. USA* **111**, 3239–3244 (2014).
22. Howden, S. M. et al. Adapting agriculture to climate change. *Proc. Natl Acad. Sci. USA* **104**, 19691–19696 (2007).
23. Li, L. et al. Insights into progress of wheat breeding in arid and infertile areas of China in the last 14 years. *Field Crops Res.* **306**, 109220 (2024).
24. Han, J., Yu, X., Chang, J., Yang, G. & He, G. Overview of the wheat genetic transformation and breeding status in China. *Methods Mol. Biol.* **1679**, 37–60 (2017).
25. Zhao, N. & Liu, B. Research of the damage and prevention measures of the wheat dry–hot wind in China [in Chinese]. *J. Agric. Catastrophol.* **1**, 68–73 (2011).
26. Jiang, T. et al. Identifying sources of uncertainty in wheat production projections with consideration of crop climatic suitability under future climate. *Agric. For. Meteorol.* **319**, 108933 (2022).
27. Wang, B. et al. Sources of uncertainty for wheat yield projections under future climate are site-specific. *Nat. Food* **1**, 720–728 (2020).
28. Wang, B. et al. Pathways to identify and reduce uncertainties in agricultural climate impact assessments. *Nat. Food* **5**, 550–556 (2024).
29. Asseng, S. et al. Uncertainty in simulating wheat yields under climate change. *Nat. Clim. Change* **3**, 827–832 (2013).
30. Lobell, D. B. et al. Greater sensitivity to drought accompanies maize yield increase in the U.S. Midwest. *Science* **344**, 516–519 (2014).
31. Lobell, D. B., Deines, J. M. & Tommaso, S. D. Changes in the drought sensitivity of US maize yields. *Nat. Food* **1**, 729–735 (2020).
32. Yang, Y. Influences and prevention measures droughts & of floods, dry–hot–wind on wheat production in Fuyang area of Anhui province [in Chinese]. *J. Agric. Catastrophol.* **4**, 45–47 (2014).
33. Zhao, J., Zhao, Y., Guo, J. & Fang, S. Spatial-temporal changes of dry–hot wind for winter wheat in Huanghuaihai Plain during the past 50 years [in Chinese]. *Sci. Agric. Sin.* **45**, 2815–2825 (2012).
34. Zhang, R., Zhang, S., Luo, J., Han, Y. & Zhang, J. Analysis of near-surface wind speed change in China during 1958–2015. *Theor. Appl. Climatol.* **137**, 2785–2801 (2019).
35. Guo, H., Xu, M. & Hu, Q. Changes in near-surface wind speed in China: 1969-2005. *Int. J. Climatol.* **31**, 349–358 (2011).
36. Lin, C., Yang, K., Qin, J. & Fu, R. Observed coherent trends of surface and upper-air wind speed over China since 1960. *J. Clim.* **26**, 2891–2903 (2013).
37. Ge, J., Feng, D., You, Q., Zhang, W. & Zhang, Y. Characteristics and causes of surface wind speed variations in Northwest China from 1979 to 2019. *Atmos. Res.* **254**, 105527 (2021).
38. Rezaei, E. E. et al. Climate change impacts on crop yields. *Nat. Rev. Earth Environ.* **4**, 831–846 (2023).
39. Xu, Y. et al. Effect of dry–hot wind on grain weight of winter wheat at different spikelet and grain positions [in Chinese]. *Chin. J. Agrometeorol.* **42**, 583 (2021).

40. Jiang, T., He, L., Feng, H., He, J. & Yu, Q. Understanding the impacts of extreme temperature and humidity compounds on winter wheat traits in China. *Agric. For. Meteorol.* **362**, 110354 (2025).
41. Vogel, E. et al. The effects of climate extremes on global agricultural yields. *Environ. Res. Lett.* **14**, 054010 (2019).
42. Hamed, R., Van Loon, A. F., Aerts, J. & Coumou, D. Impacts of compound hot–dry extremes on US soybean yields. *Earth Syst. Dyn.* **12**, 1371–1391 (2021).
43. Matiu, M., Ankerst, D. P. & Menzel, A. Interactions between temperature and drought in global and regional crop yield variability during 1961-2014. *PLoS ONE* **12**, e0178339 (2017).
44. Hultgren, A. et al. Impacts of climate change on global agriculture accounting for adaptation. *Nature* **642**, 644–652 (2025).
45. Zhang, Y. et al. Progress in genetic improvement of grain yield and related physiological traits of Chinese wheat in Henan Province. *Field Crops Res.* **199**, 117–128 (2016).
46. Li, H. et al. Wheat breeding in northern China: achievements and technical advances. *Crop J.* **7**, 718–729 (2019).
47. Zhang, Z. et al. Decadal changes in wind speed have offset and then aggravated the impact of warming on maize production in China since 1980. *Nat. Commun.* **16**, 9739 (2025).
48. National Bureau of Statistics of China *China Statistical Yearbook 2018* (China Statistics Press, 2018).
49. Cheng, C. S. et al. Reconstruction of near-surface hourly wind speed data sets during the period 1959–2021 over China. *Earth Space Sci.* **10**, e2023EA003295 (2023).
50. He, J. et al. The first high-resolution meteorological forcing dataset for land process studies over China. *Sci. Data* **7**, 25 (2020).
51. He, J. et al. China meteorological forcing dataset v2.0 (1951–2024). *National Tibetan Plateau/ Third Pole Environment Data Center* https://doi.org/10.11888/Atmos.tpdc.302088 (2024).
52. Liu, Y. et al. Development of a daily multilayer cropland soil moisture dataset for China using machine learning and application to cropping patterns. *J. Hydrometeorol.* **22**, 445–461 (2021).
53. Cheng, F. et al. ChinaCropSM1 km: a fine 1 km daily soil moisture dataset for dryland wheat and maize across China during 1993–2018. *Earth Syst. Sci. Data* **15**, 395–409 (2023).
54. Department of Price of the National Development and Reform Commission *National Compilation of Cost-Benefit Data of Agricultural Products 2018 [in Chinese]* (China Statistics Press, 2018).
55. Xie, W. et al. Crop switching can enhance environmental sustainability and farmer incomes in China. *Nature* **616**, 300–305 (2023).
56. Cheng, C. S. Reconstruction of near-surface hourly wind speed datasets during the period 1959–2021 over China. *Zenodo* https://doi.org/10.5281/zenodo.8350860 (2023).
57. Cheng, F. et al. ChinaCropSM1km: a fine 1km daily soil moisture dataset for dryland wheat and maize across China during 1993–2018 (versions wheat0–10cm). *Zenodo* https://doi.org/10.5281/zenodo.6834530 (2022).
58. Cheng, F. et al. ChinaCropSM1km: a fine 1km daily soil moisture dataset for dryland wheat and maize across China during 1993–2018 (versions wheat10–20cm). *Zenodo* https://doi.org/10.5281/zenodo.6822591 (2022).
59. Jiang, T. et al. Code for "Wheat yield sensitivity to compound hot–dry–windy events is increasing in China". *figshare* https://doi.org/10.6084/m9.figshare.33653194 (2026).

Author contributions

T.J. and H.M. designed the study. T.J. performed statistical analyses, calculated the results and drafted the paper. T.J., H.M. and N.Y. provided crop, soil moisture and climate data. B.W., Z.H., X.R., N.Y., K.G., H.F., J.H. and Q.Y. advised on the interpretation of the results and revised the paper.

Funding

This research was supported by the Key Research and Development Program of Shaanxi (number 2023-ZDLNY-64), the National Natural Science Foundation of China (U2243235), Shaanxi Province 'San-qin Scholars' innovation team Support Plan—Northwest A&F University Smart Agriculture Innovation Team and Shaanxi Postdoctoral Research Project (2023BSHEDZZ133) and Henan Province International Science and Technology Cooperation Project (project number 262102521005).

Competing interests

The authors declare no competing interests.

Additional information

Supplementary information The online version contains supplementary material available at https://doi.org/10.1038/s43016-026-01452-8.

Correspondence and requests for materials should be addressed to Tengcong Jiang, Qiang Yu or Haijiao Ma.

Peer review information *Nature Food* thanks Raed Hamed, Xiaomao Lin and Peijun Shi for their contribution to the peer review of this work.

Reprints and permissions information is available at www.nature.com/reprints.

Publisher's note Springer Nature remains neutral with regard to jurisdictional claims in published maps and institutional affiliations.

Springer Nature or its licensor (e.g. a society or other partner) holds exclusive rights to this article under a publishing agreement with the author(s) or other rightsholder(s); author self-archiving of the accepted manuscript version of this article is solely governed by the terms of such publishing agreement and applicable law.

© The Author(s), under exclusive licence to Springer Nature Limited 2026

nature portfolio

Corresponding author(s): Tengcong Jiang, Qiang Yu and Haijiao Ma.

Last updated by author(s): Sep 13, 2026

Reporting Summary

Nature Portfolio wishes to improve the reproducibility of the work that we publish. This form provides structure for consistency and transparency in reporting. For further information on Nature Portfolio policies, see our Editorial Policies and the Editorial Policy Checklist.

Statistics

For all statistical analyses, confirm that the following items are present in the figure legend, table legend, main text, or Methods section.

n/a	Confirmed
☐	☒ The exact sample size (*n*) for each experimental group/condition, given as a discrete number and unit of measurement
☐	☒ A statement on whether measurements were taken from distinct samples or whether the same sample was measured repeatedly
☐	☒ The statistical test(s) used AND whether they are one- or two-sided *Only common tests should be described solely by name; describe more complex techniques in the Methods section.*
☐	☒ A description of all covariates tested
☐	☒ A description of any assumptions or corrections, such as tests of normality and adjustment for multiple comparisons
☐	☒ A full description of the statistical parameters including central tendency (e.g. means) or other basic estimates (e.g. regression coefficient) AND variation (e.g. standard deviation) or associated estimates of uncertainty (e.g. confidence intervals)
☐	☒ For null hypothesis testing, the test statistic (e.g. *F*, *t*, *r*) with confidence intervals, effect sizes, degrees of freedom and *P* value noted *Give P values as exact values whenever suitable.*
☒	☐ For Bayesian analysis, information on the choice of priors and Markov chain Monte Carlo settings
☐	☒ For hierarchical and complex designs, identification of the appropriate level for tests and full reporting of outcomes
☐	☒ Estimates of effect sizes (e.g. Cohen's *d*, Pearson's *r*), indicating how they were calculated

Our web collection on statistics for biologists contains articles on many of the points above.

Software and code

Policy information about availability of computer code

Data collection	We used open source software R version 4.5.3, RStudio version 2026.01.1+403, and Microsoft Excel for data collection.
Data analysis	Data analysis, including trend analysis, regression, machine learning, and visualization, was conducted using custom R scripts developed by the authors. Specific R packages were employed for various tasks: "tidyverse" for data integration, "sf" for spatial data analysis, "RandomForest" for estimating county-level phenology, "fixest" for fixed-effects modeling, and "ggplot2" for data visualization. All R scripts have been deposited in a publicly accessible repository at (https://github.com/Jhone-FML/Crop-yield-loss-at-HDW) and (https://doi.org/10.6084/m9.figshare.33653194).

For manuscripts utilizing custom algorithms or software that are central to the research but not yet described in published literature, software must be made available to editors and reviewers. We strongly encourage code deposition in a community repository (e.g. GitHub). See the Nature Portfolio guidelines for submitting code & software for further information.

Data

Policy information about availability of data

All manuscripts must include a data availability statement. This statement should provide the following information, where applicable:

- Accession codes, unique identifiers, or web links for publicly available datasets
- A description of any restrictions on data availability
- For clinical datasets or third party data, please ensure that the statement adheres to our policy

Publicly available environmental data were obtained from the following repositories: ERA5-Land hourly 2-m air temperature from the Copernicus Climate Data Store (https://doi.org/10.24381/cds.e2161bac); reconstructed hourly 10-m wind speed for China from Zenodo (https://doi.org/10.5281/zenodo.8350860); three-hourly relative humidity and daily precipitation from the China Meteorological Forcing Dataset v2.0 at the National Tibetan Plateau/Third Pole Environment Data Center (https://doi.org/10.11888/Atmos.tpdc.302088); SMML-CHN v1.0 soil moisture from the NASA Aura Validation Data Center (https://avdc.gsfc.nasa.gov/pub/data/project/SMML_CHN/); and the wheat 0–20-cm daily soil moisture from Zenodo (https://doi.org/10.5281/zenodo.6834530 and https://zenodo.org/records/6822591). County-level wheat-yield records were compiled from national, provincial and county statistical yearbooks. Crop-phenology observations were obtained from the China Meteorological Administration Data Service Centre (https://data.cma.cn/). Provincial wheat production-cost records were compiled from annual editions of the National Compilation of Cost-Benefit Data of Agricultural Products published by the National Development and Reform Commission and China Statistics Press. Provincial wheat production-cost records are available via figshare at https://doi.org/10.6084/m9.figshare.33653194 (ref. 57). National wheat variety-trial records were obtained through the National Crop Variety Certification Committee evaluation process. The National wheat variety-trial records and compiled county-level wheat-yield are are available from the corresponding author, Tengcong Jiang (tongcong_jiang@nwafu.edu.cn), upon request.

Research involving human participants, their data, or biological material

Policy information about studies with human participants or human data. See also policy information about sex, gender (identity/presentation), and sexual orientation and race, ethnicity and racism.

Reporting on sex and gender	Not applicable
Reporting on race, ethnicity, or other socially relevant groupings	Not applicable
Population characteristics	Not applicable
Recruitment	Not applicable
Ethics oversight	Not applicable

Note that full information on the approval of the study protocol must also be provided in the manuscript.

Field-specific reporting

Please select the one below that is the best fit for your research. If you are not sure, read the appropriate sections before making your selection.

☐ Life sciences ☐ Behavioural & social sciences ☒ Ecological, evolutionary & environmental sciences

For a reference copy of the document with all sections, see nature.com/documents/nr-reporting-summary-flat.pdf

Ecological, evolutionary & environmental sciences study design

All studies must disclose on these points even when the disclosure is negative.

Study description	In this study, using 32,318 county-level yield records, phenology data spanning 7413 station-years (1981-2018)6,525 field trials from the national wheat variety certification program, and high-resolution reanalyzed climate and soil water datasets, and wheat production costs dataset (1981-2018: fertilization, irrigation, mechanization, and seed), we employed mixed linear models to analyze yield responses. Our results demonstrate that high-temperature, low-humidity dry-hot winds consistently cause the most significant yield losses, with reductions of up to 7.5% and 12.7% per standardized unit (10.0 hours) of exposure, based on county-level and field trial data, respectively. Its increasing trend (0.7 hours dec-1), driven by declining relative humidity and advancing phenology, strengthened negative yield sensitivity, with changes of -33.0~13.1 kg ha-1 hour-1 at the field scale and -31.5~-15.6 kg ha-1 hour-1 at the county scale.
Research sample	This study leveraged extensive datasets to analyze wheat yield sensitivity to dry-hot winds. County-level yield data from 898 counties between 1981 and 2018 included 32,318 county-year records. Field trial data, reflecting the distribution of wheat-producing regions, were drawn from 77 sites covering 460 wheat varieties during 2007–2018, yielding 6,525 site-variety-year records of yield and phenological data. Additionally, phenological data spanning 1981–2018 were collected from 352 sites, encompassing 7,435 station-year observations. Meteorological variables, including 2-meter air temperature and dew point temperature (T and Td, °C), 10-meter wind speed (W, m s^{-1}), and relative humidity (%), were derived from the ERA5, RNSHWD, reanalysis dataset at a 0.25-degree spatial resolution, respectively. Data were extracted using the geographic centroids of counties. Soil moisture were derive from two

complementary datasets (1981-1992: https://avdc.gsfc.nasa.gov/pub/data/project/SMML_CHN/ and 1993-2018: https://nesdc.org.cn/theme/index?projectId=63dc6c627e281740ae0f287f), covering depth of -20 cm—provided additional context for assessing environmental conditions. Wheat production cost data (fertilization, irrigation, mechanization, and seed) for 1981-2018 were extracted from the Cost-benefit of Agricultural Products in China, provided additional context for assessing technological progress.

Sampling strategy

No statistical methods were used to predetermine sample size. Sample sizes were determined by the availability of historical records meeting the data requirements of the analyses. The spatial and temporal coverage of the datasets provided variation for estimating yield responses within the fixed-effects framework. Bootstrap confidence intervals were used to quantify the precision of the estimates. The county-level sample size (898) was determined based on the spatial distribution of China's major wheat-growing regions. The time span (1981–2018) was defined by the intersection of the years with recorded yields (1981–2022) and those with phenological observation data from the network (1980–2018). For the field trial data, the site sample size (74) was identified through the intersection of the overall distribution of field trial stations and the distribution of major wheat-growing regions. The time span (2007–2018) and the number of wheat varieties (673) were determined based on the observation period and variety coverage of the selected sites. Reanalyzed meteorological and soil moisture data were analyzed at an hourly resolution to ensure that the statistical models could estimate the short-term (within a few hours or daily) impact of dry-hot winds on crops. Additionally, soil moisture was divided into three growth stages for the varying sensitivity of wheat to soil moisture at different stages of wheat.

Data collection

The authors compiled existing datasets for this analysis. County-level wheat-yield records were obtained from national, provincial and county statistical yearbooks, and national wheat variety-trial records were obtained through the National Crop Variety Certification Committee evaluation process. Environmental data were obtained from ERA5-Land, the reconstructed hourly wind-speed dataset for China, CMFD v2.0 and published soil-moisture datasets. Phenology observations were obtained from the China Meteorological Administration, and provincial production-cost records were compiled from the National Compilation of Cost-Benefit Data of Agricultural Products. Sources and access conditions are provided in the Data Availability statement.
H.M. provided statistical yearbook data from the China Statistical Yearbook Database (https://www.stats.gov.cn/sj/ndsj/), extracting county-level wheat yield data for major wheat-producing provinces in China from 1981 to 2018. H. M. collected wheat production cost data (fertilization, irrigation, mechanization, and seed) for 1981-2018 were extracted from the Cost-benefit of Agricultural Products in China. H.M. collected yield and phenological data from the China Wheat Regional Trial dataset, based on national wheat variety certification trials. H.M. also provided phenological data for 1981–2018 sourced from the China Meteorological Administration (https://data.cma.cn/). T.J. contributed climate and soil moisture. Additionally, T.J. integrated and paired the datasets for analysis.

Timing and spatial scale

The spatial extent of wheat yield data covers the northern wheat-producing regions of China, spanning 1981–2018, with a spatial resolution at the county level. The spatial extent of phenological data also encompasses the northern wheat-producing regions of China, covering the same time span (1981–2018) with a spatial resolution at the station level. Field trial data are limited to the northern wheat-producing regions of China, spanning 2007–2018, with a spatial resolution at the station level. Reanalyzed meteorological and soil data were selected for the northern wheat-producing regions of China, covering 1981–2018, with a spatial resolution of 0.25 degrees. The spatial extent of wheat production cost dataset covers the northern wheat-producing regions of China, spanning 1981–2018, with a spatial resolution at the provience level.

Data exclusions

We filtered the county-level yield data, excluding outliers that were either an order of magnitude lower or higher than the average yield (accounting for less than 1% of the samples).

Reproducibility

All analyses were based on real data and standard statistical approaches, such as trend analysis, machine learning analysis, and fixed-effects model analysis. findings can be reproduced and repeated if following the method accordingly.

Randomization

Randomization is not relevant to this study, as no treatment is applied.

Blinding

Blinding is not relevant to this study, as no treatment is applied.

Did the study involve field work? ☐ Yes ☒ No

Reporting for specific materials, systems and methods

We require information from authors about some types of materials, experimental systems and methods used in many studies. Here, indicate whether each material, system or method listed is relevant to your study. If you are not sure if a list item applies to your research, read the appropriate section before selecting a response.

Materials & experimental systems

n/a	Involved in the study
☒	☐ Antibodies
☒	☐ Eukaryotic cell lines
☒	☐ Palaeontology and archaeology
☒	☐ Animals and other organisms
☒	☐ Clinical data
☒	☐ Dual use research of concern
☒	☐ Plants

Methods

n/a	Involved in the study
☒	☐ ChIP-seq
☒	☐ Flow cytometry
☒	☐ MRI-based neuroimaging

Plants

Seed stocks	NA
Novel plant genotypes	NA
Authentication	NA